Bioinorganic Chemistry Very Important Paper

DOI: 10.1002/anie.201403402

Decay of Iron(V) Nitride Complexes By a N–N Bond-Coupling Reaction in Solution: A Combined Spectroscopic and Theoretical Analysis**

*Oliver Krahe, Eckhard Bill, and Frank Neese**

Dedicated to the MPI für Kohlenforschung on the occasion of its centenary

Abstract: *Cryogenically trapped Fe^{V} nitride complexes with cyclam-based ligands were found to decay by bimolecular reactions, forming exclusively Fe^{II} compounds. Characterization of educts and products by Mössbauer spectroscopy, mass spectrometry, and spectroscopy-oriented DFT calculations showed that the reaction mechanism is reductive nitride coupling and release of dinitrogen ($2\,Fe^{V}\equiv N \rightarrow Fe^{II}\text{-}N{=}N\text{-}Fe^{II} \rightarrow 2\,Fe^{II} + N_2$). The reaction pathways, representing an "inverse" of the Haber–Bosch reaction, were computationally explored in detail, also to judge the feasibility of yielding catalytically competent $Fe^{V}(N)$. Implications for the photolytic cleavage of Fe^{III} azides used to generate high-valent Fe nitrides are discussed.*

High-valent iron nitride centers are of crucial interest as key intermediates in complex chemical processes, such as nitrogen fixation in nature[1] and industry.[2] The reactive species are challenging to study in technical or biological environments, but various iron nitride complexes have been synthesized in the oxidation states IV, V, and VI to model the possible atomic and electronic structures as well as reaction pathways.[3] A variety of ligands was explored which impose four-, five-, or six-coordination on the iron centers with trigonal/tetrahedral,[3b,c,e,h,4] square-pyramidal,[3g] and octahedral coordination geometries.[3d,f,5]

Tetrahedral Fe^{IV} nitride complexes with bulky trigonal ligands could be synthesized in solution and even isolated.[3a,6] Their reactivity was systematically surveyed for a number of transformations.[3h,6a,7] The tetrahedral Fe^{IV} nitride groups were found to at least partially decay by intermolecular reductive N–N coupling yielding Fe^{I}-NN-Fe^{I} dimers, provided the steric demand of ligand does not prevent such bimolecular reactions.[3e,8]

In contrast, the reactivity of Fe^{V} nitrides is more challenging to study and less well understood owing to their fleeting nature. Recently, synthesis and structural characterization of the first Fe^{V} nitride with a tripodal N-heterocyclic carbene (NHC) ligand was reported, which showed for example, formation of ammonia from water.[3b] However, tetragonal Fe^{V} nitrides could not be isolated, but were rather generated at cryogenic temperatures in frozen solutions by photolysis of Fe^{III} azide precursors. Spectroscopic analysis yielded much insight in their electronic structures,[3d,f,g,5b,6a] whereas reactivity studies are scarce. Reactions with phosphine was monitored by time-resolved IR spectroscopy,[9] and the tetragonal $[Fe^{V}(N)\text{cyc-ac}]^{+}$ ion (**1b**) (cyc-ac = 1,4,8,11-tetraazacyclotetradecane-1-acetate) was studied in the gas phase. However, C–H bond activation was not observed in these experiments.[10]

Herein we demonstrate that cryogenically trapped, cyclam-based tetragonal Fe^{V} nitride complexes decay, upon melting of their frozen solvent matrix, in bimolecular reactions, forming exclusively Fe^{II} compounds. The mechanism is reductive nitride coupling and release of dinitrogen (i.e., $2\,Fe^{V}\equiv N \rightarrow Fe^{II}\text{-}N{=}N\text{-}Fe^{II} \rightarrow 2\,Fe^{II} + N_2$). The reaction is interesting not only because it represents an "inverse" of the Haber–Bosch reaction, such that the converse of the six-electron redox process would yield catalytically competent $Fe^{V}(N)$, but the feasibility of reaction also has implications for the photolytic cleavage of Fe^{III} azides used to generate high-valent Fe nitrides.

High-valent $[Fe^{V}(N)\text{cyc-ac}]PF_6$ (**1b**) was obtained from the Fe^{III} azide complex $[Fe^{III}(N_3)\text{cyc-ac}]PF_6$ (**1**) by preparative photolysis in frozen solution at 77 K with visible light (Scheme 1).[3d,f,5b] Mössbauer spectra were recorded before and after photolysis, demonstrating high yields of the $Fe^{V}N$ target species (87% **1b**, Figure S1 in the Supporting Information). Photoreduction (i.e. $Fe^{III}N_3 + h\nu \rightarrow Fe^{II} + N_3^{\bullet}$)[3f] was negligible as possible contributions of Fe^{II} species to the

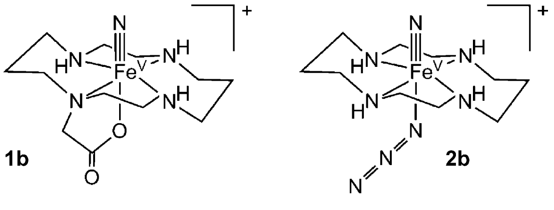

Scheme 1. $Fe^{V}N$ complexes **1b**[3d,f] and **2b**.[5b]

---

[*] O. Krahe, Dr. E. Bill, Prof. Dr. F. Neese
Max-Planck Institute for Chemical Energy Conversion
Stiftstrasse 34–36, 45470 Mülheim an der Ruhr (Germany)
E-mail: Frank.Neese@cec.mpg.de
Homepage: http://www.cec.mpg.de

[**] We thank Petra Höfer for her assistance with the electrochemical measurements, Dr. Wolfgang Schrader for his support in the mass spectrometry study and the Max-Planck society for financial support. This work was initiated in the framework of the SFB 813 (University of Bonn).

Supporting information for this article is available on the WWW under http://dx.doi.org/10.1002/anie.201403402.

Mössbauer spectra were below the detection limit. The photolyzed sample was subsequently allowed to thaw in an argon atmosphere before it was refrozen again in liquid nitrogen (timescale ≈ 5 min). Mössbauer spectra recorded thereafter (Figure 1 A) demonstrate complete decay of the Fe^{V} nitride **1b** and exclusive formation of a single new species (**1d**) with Mössbauer parameters $\delta = 0.57\,\mathrm{mm\,s^{-1}}$ and $\Delta E_Q = 0.59\,\mathrm{mm\,s^{-1}}$. Remarkably, the fraction of residual Fe^{III}N$_3$ starting material remaining from incomplete primary photolysis (13%) was not affected by the thaw/freeze procedure. We conclude that the Fe^{V}N complex **1b** does not oxidize the Fe^{III} precursor **1** or undergo any other reaction with it.

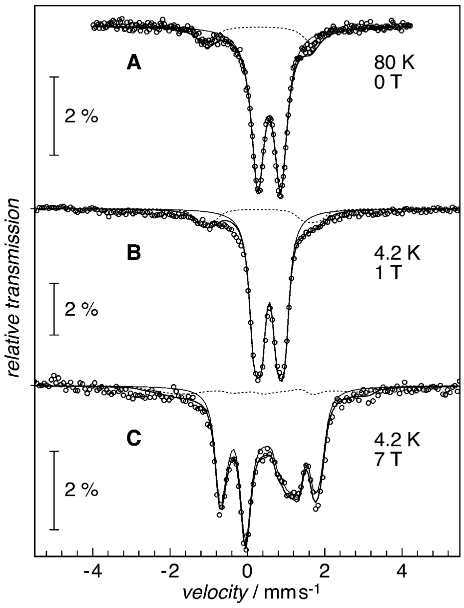

Figure 1. Zero-field Mössbauer spectra of the decay product of Fe^{V} nitride **1b** recorded at A) 80 K and B) 4.2 K with 1 T and C) 7 T (applied field. The thin solid trace is a simulation for [Fe^{II}(cyclam-ac) (MeCN)]$^+$ **1d** with $S = 0$ (87%, Table 1), and the dotted line is a spin-Hamiltonian simulation with $S = 1/2$ for the remaining non-photolyzed Fe^{III} complex **1** with parameters taken from Ref. [3f] (details in Table S1).

The low quadrupole splitting and moderate isomer shift of the decay product **1d** is consistent with either high-spin Fe^{III} or low-spin Fe^{II} iron.[3f,5b] Magnetic Mössbauer measurements rule out Fe^{III}, because the new species is diamagnetic (Figure 1 B,C). Hence, **1d** must be a low-spin Fe^{II} complex. Nearly identical Mössbauer spectra have been obtained from electrochemically reduced (**1**)[3f] and (**2**)[5b] ($\delta = 0.55\,\mathrm{mm\,s^{-1}}$, $\Delta E_Q = 0.72\,\mathrm{mm\,s^{-1}}$). We suggest to formulate **1d** as six-coordinate [Fe^{II}(cyc-ac)(MeCN)]$^+$ with an acetonitrile molecule (MeCN) bound in axial position, since the low-spin state requires a strong ligand field. Density functional theory (DFT) calculations support this conclusion since the calculated Mössbauer parameters for an optimized quasi-octahedral Fe^{II} low-spin structure of **1d** (Table 1) are in excellent agreement with experiment.

Table 1: Experimental and calculated Mössbauer parameters.

Complex	Experimental δ	Experimental ΔE_Q [mm s^{-1}]	Experimental η	Calculated δ	Calculated ΔE_Q [mm s^{-1}]	Calculated η
[Fe^{III}(N$_3$)cyc-ac]$^+$ (**1**)	0.27	−2.48	0.42	0.26	−2.36	0.27
[Fe^{V}(N)cyc-ac]$^+$ (**1b**)	−0.01	1.58		−0.11	−1.89	0.61
(N$_2$)[Fe^{II}(cyc-ac)]$_2$$^{2+}$ (**1c**)				0.44	+0.78	0.26
[Fe^{II}(MeCN)cyc-ac]$^+$ (**1d**)	0.57	0.59	0.4	0.54	+0.42	0.41
	0.56[a]	0.54[a]				
“[Fe^{II}(N$_3$)cyc-ac]”	0.56[a]	0.54[a]		0.64	+0.66	0.29
(N$_2$)[Fe^{II}(cyc)(N$_3$)]$^{2+}$(**2c**)				0.39	+0.73	0.21
[Fe^{II}(MeCN)(N$_3$)cyc]$^+$ (**2d**)	0.55[b]	0.72[b]		0.55	+0.66	0.12
“[Fe^{II}(N$_3$)$_2$cyc]”	0.55[b]	0.72[b]		0.65	+0.84	0.19

[a] Electrochemically reduced (**2**), data from Ref. [3f]. [b] From Ref. [5b].

The Mössbauer and DFT results demonstrate that the Fe^{V} nitride **1b** decays differently in solution than in the gas phase. For the gas phase, only formation of Fe^{III} products has been detected and was explained by intramolecular decomposition through ligand degradation.[10] In solution (1 mM) collisions of complex cations are more than in low-pressure gas atmosphere. Hence intermolecular reactions of the high-valent species are favored over intramolecular decomposition. We will show below that the corresponding reaction mechanism is nitride coupling.

The Fe^{V} nitride complex **2b** generated from bis(azide) [Fe(N$_3$)$_2$cyc]$^+$ (**2**) also forms a Fe^{II} species upon thawing (**2d**, $\delta = 0.55\,\mathrm{mm\,s^{-1}}$ and $\Delta E_Q = 0.72\,\mathrm{mm\,s^{-1}}$).[5b] For this species, the nature of the sixth axial ligand, MeCN or N$_3^-$, has been the subject of discussion.[3f,5b] Calculated Mössbauer parameters given in Table 1 now clearly support the formulation [Fe^{II}(N$_3$)(MeCN)cyc]$^+$ with a coordinated acetonitrile molecule. Thus, similar decay processes can be assumed for **1b** and **2b**, yielding similar six-coordinated Fe^{II} low-spin products with MeCN bound as axial ligand.

The corresponding replacement of an apical azide anion by a neutral solvent molecule upon reduction of Fe^{III} **1** and **2** was independently probed by IR-spectro-electrochemistry. Complex **1** in acetonitrile shows a non-symmetric azide stretching vibration at 2053 cm^{-1} that disappeared upon the reversible one-electron reduction, while a new band appeared at 2006 cm^{-1} (for details see Supporting Information). In parallel, the carbonyl stretching vibration shifted from 1688 cm^{-1} to 1636 cm^{-1}, which agrees with our previous theoretical IR band assignment for the [Fe^{II}(MeCN)cyc-ac]$^+$ complex, observed in a time-resolved IR investigation of **1**.[11] Interestingly, the azide band of the bis(azide) Fe^{III} complex **2**, found at 2042 cm^{-1} decreased only by around 50% in intensity while the same new band as found for **1** evolved at 2006 cm^{-1} (see Figure S3, S4). Since 2006 cm^{-1} is the IR stretching energy of free azide anions in acetonitrile solution (see IR spectrum in the Supporting Information), we conclude that **1** and **2**, both, release an azide anion upon reduction, but the second azide of **2** remains bound as the fifth ligand. DFT calculations support this interpretation since a single azide stretching vibration at 2053 cm^{-1} is predicted for the Fe^{III} state (2053 cm^{-1} for **1** as well). This result is reasonably close to experiment, whereas the band for reduced [Fe^{II}(N$_3$)(MeCN)cyc]$^+$ (**2d**) should be theoretically shifted by about 9 cm^{-1} to 2062 cm^{-1}, which was experimentally not resolved (bandwidth $>20\ cm^{-1}$).

Table 2: Dinitrogen isotope pattern obtained from melting samples of photolyzed **1** and **2** by EI-MS measurements.

	Natural abundance [%]	calcd [%]	Observed for **1** $[Fe(N)cycl\text{-}ac]^+$ [%]	Observed for **2** $[Fe(N)(N_3)cycl]^+$ [%]
$^{14}N^{14}N$	99.2813	41.7	73.9	82.2
$^{15}N^{14}N$	0.7174	50.0	22.2	15.4
$^{15}N^{15}N$	0.0013	8.3	3.9	2.5

Thus, the Mössbauer, IR and DFT data show that the Fe^{II} decay products **1d** and **2d** of the Fe^{V} nitrides **1b** and **2b** are the well-defined complexes $[Fe^{II}(MeCN)cyc\text{-}ac]^+$ and $[Fe^{II}(N_3)(MeCN)cyc]^+$, respectively. Mass spectrometry with ^{15}N-labeled complexes strongly supports the interpretation that these species are formed by intermolecular nitride coupling and decay of the short-lived dinuclear Fe^{II}-NN-Fe^{II} intermediate. Since commercially enriched azide features 100% single terminal ^{15}N labels, the resulting Fe^{III} starting material has two isotopes, as shown in Scheme 2. Oxidative photo-cleavage of the bound azides therefore yields equal amounts of $Fe^{V}(^{14}N)$ and $Fe^{V}(^{15}N)$, as well as $^{14}N^{14}N$ and $^{15}N^{14}N$.

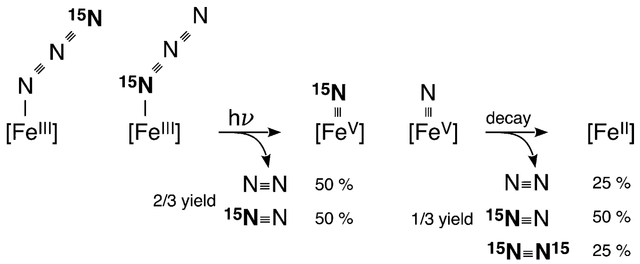

Scheme 2. Proposed decay pathway with ^{15}N isotope labeling.

Subsequent nitride coupling and decay of the resulting Fe^{II}-NN-Fe^{II} intermediate during melting of the samples leads to the same N_2 isotopes, albeit in different yields. However, in addition, doubly labeled $^{15}N^{15}N$ is generated upon dimerization of two $Fe^{V}(^{15}N)$ groups (Scheme 2). In the actual reaction assay this is the only conceivable pathway for linking two ^{15}N atoms. The alternative pathway through $N_3^{\bullet}$ radical coupling ($2N_3^{\bullet} \rightarrow 3N_2$) is excluded as the absence of Fe^{II} photoproducts also rules out $N_3^{\bullet}$ production by reductive $Fe^{III}N_3$ cleavage, that is, the reaction $Fe^{III}N_3 \rightarrow Fe^{II} + N_3^{\bullet}$ is not observed.

We performed EI-MS measurements to monitor the gas released from ^{15}N-labeled **1** and **2** upon melting after photo-oxidation in frozen solution at 80 K. Although the spectrometer could not be completely purged from atmospheric N_2, the possible background of naturally abundant $^{14}N^{15}N$ (0.7%) and $^{15}N^{15}N$ (0.001%) was negligible compared to the large relative fractions expected for the reaction gas, which are 50% $^{14}N^{15}N$, 41.7% $^{14}N^{14}N$, and 8.3% $^{15}N^{15}N$ (yields were estimated from combined conversion ratios of the photolysis and the nitride coupling). Although the dilution with atmospheric N_2 lowered the actual yield of labeled dinitrogen from samples of treated **1** and **2** (Table 2), the high fraction of 3.9% $^{15}N^{15}N$ found for **1b** (2.5% for **2b**) clearly exceeded the detection limit of the instrument (details in the Supporting Information). This demonstrates that nitride coupling is the decay mechanism of cyclam $Fe^{V}N$ complexes.

For deeper understanding of the nitride decay pathway and its driving force, we performed DFT calculations. The calculated energy profiles are very similar for **1b** and **2b** (see Scheme 3). To show that the presented decay pathway is energetically the most favorable one, other feasible reactions with the solvent (acetonitrile) were investigated computationally as well.

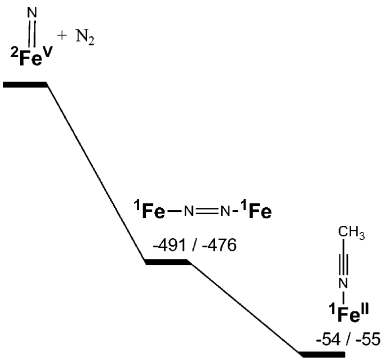

Scheme 3. Calculated reaction pathway for **1b/2b**, spin multiplicity of Iron as ^{n}Fe superscript, energies in $kJ\,mol^{-1}$.

The dimerization of the Fe^{V} nitrides by nitrogen coupling is calculated to be strongly exergonic ($-491\ kJ\,mol^{-1}$ for **1b** and $-476\ kJ\,mol^{-1}$ for **2b**). Owing to the change in spin state (from triplet to singlet) we were not able to locate a transition state for the iron nitride dimerization; the energy difference between $S=1$ and $S=0$ is 66 $kJ\,mol^{-1}$ for **1c** and 89 $kJ\,mol^{-1}$ for **2c**. However, relaxed surface scans on the singlet and triplet surfaces along the nitrogen–nitrogen bond show a decrease in energy for this reaction without any discernible barrier (Figure S6 and S7). The dinitrogen bridged Fe^{II} dimer shows a nitrogen–nitrogen bond length of 1.158 Å for **1c** dimer and 1.161 Å for **2c**, while the bond for free N_2 is calculated to be 1.102 Å. Hence, the N–N bond is slightly elongated in this intermediate.

The large driving force for the dimerization can be rationalized by assuming that the Fe–N bond is a resonance of the type $Fe^{V}(S_{Fe}=1/2)N^{3-} \leftrightarrow Fe^{II}(S_{Fe}=0)N^{\bullet}(S_N=1/2)$.[3d] Reasoning from the nitride-radical resonance structure, the dimerization might be regarded as a radical coupling that proceeds in a barrier-free fashion. The stability of the dimeric intermediate might even be the driving force for the $Fe^{V}N$ decay since the dinitrogen bridged dinuclear iron(II) complex can be assumed to be relatively unstable in coordinating solvents. Dissociation and coordination of an acetonitrile solvent molecule should be fast and is calculated to be exothermic by about $-54\,\mathrm{kJ\,mol^{-1}}$ (**1d**) and $-55\,\mathrm{kJ\,mol^{-1}}$ (**2d**).

Since the described reaction appears to proceed without any barrier and is extremely exothermic, competing reactions are unlikely. This is in good agreement with the very clean formation of the $\mathrm{Fe^{II}}$ complex observed in the Mössbauer spectra without detectable side products. To validate this assumption we considered possible reactions with the solvent in our calculations.

Scheme 4 shows the reaction profile for hydrogen abstraction from acetonitrile. The calculations were performed for all hypothetically possible spin states (doublet, quartet, and sextet). The doublet transition state turns out to be the transition state that is lowest in energy. However, the value of $133\,\mathrm{kJ\,mol^{-1}}$ it is still too high to make the H atom abstraction feasible at room temperature. The overall reaction is endergonic by about $48\,\mathrm{kJ\,mol^{-1}}$ for the imido complex in its triplet ground state. All attempts to locate a transition state for a nitrogen insertion reaction into the C–H bond failed for all investigated spin states.

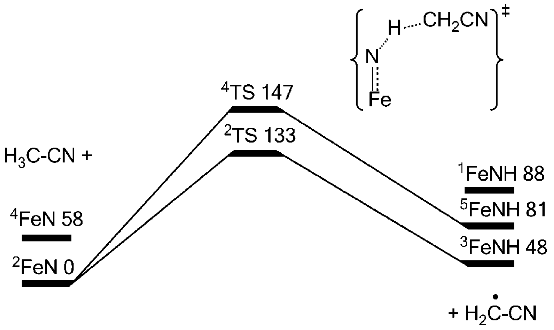

Scheme 4. Calculated C–H-activation with the solvent Acetonitrile **1b**, multiplicity as ^{n}Fe superscript, energies in $\mathrm{kJ\,mol^{-1}}$.

Another possible reaction would be the attack of the acetonitrile nitrogen on the nitrido nitrogen (see Scheme 5). Even though the reaction is calculated to be slightly exergonic ($-5\,\mathrm{kJ\,mol^{-1}}$ for the doublet state, which was calculated to be lowest in energy), the reaction barrier of $102\,\mathrm{kJ\,mol^{-1}}$ is too high to allow significant thermally activated reaction.

Although both the considered reactions of **1b** with acetonitrile have prohibitively high activation barriers, in principle they may be kinetically enabled since acetonitrile as solvent is present in very large excess. For the actual experiments however, this can be safely ruled out, as **1b** was allowed to decay at the low melting point of the reaction mixture (below −45 °C).

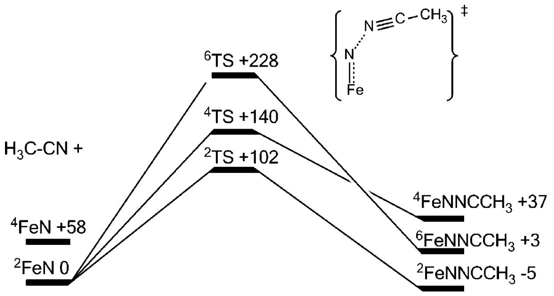

Scheme 5. Calculated coordination of acetonitrile on **1b**, spin multiplicity as ^{n}Fe superscript, energies in $\mathrm{kJ\,mol^{-1}}$.

It was discussed before, that alternatively to the photooxidation observed for **1** at 419 nm, which yields $\mathrm{Fe^{V}N}$ by N_2 elimination, the complex may also undergo wavelength-dependent photoreduction, forming $\mathrm{Fe^{II}}$ (**1d**) by $N_3^{\bullet}$ radical elimination. This was inferred from the detection of low-spin $\mathrm{Fe^{II}}$ ($\delta = 0.56\,\mathrm{mm\,s^{-1}}$ and $\Delta E_Q = 0.54\,\mathrm{mm\,s^{-1}}$, 52 % yield) after irradiation with white light or 300 nm radiation in liquid acetonitrile solution.[3f] Photolysis of **1** performed with blue 470 nm light in liquid butyronitrile under argon at −65 °C afforded even complete conversion into the reduced form **1d** ($\delta = 0.57\,\mathrm{mm\,s^{-1}}$, $\Delta E_Q = 0.57\,\mathrm{mm\,s^{-1}}$, see Figure S8). However, the melting experiments with $\mathrm{Fe^{V}}$ nitrides trapped in frozen solution indicate that primary photoreduction is not necessarily the origin of this conversion, since $\mathrm{Fe^{V}N}$ species from primary photooxidation may yield the same $\mathrm{Fe^{II}}$ product.

We also re-investigated the wavelength dependence of photolysis in frozen state, in which follow-up reactions of the primary iron photoproducts should be hampered. To this end identical samples of **1** have been illuminated at 80 K with 304 nm light instead of 470 nm as in the experiments presented above. Remarkably, the blue-shift did not change the Mössbauer spectrum qualitatively. Only the rate of photoconversion of **1** was lower, which may simply be due to the lower photon flux (Figure S1 and S2). In particular, formation of $\mathrm{Fe^{II}}$ (**1d**) through photoreduction was not detectable, as found before at 470 nm. In both cases the same $\mathrm{Fe^{V}N}$ oxidation product **1b** was found. Hence, wavelength dependence of photolysis in frozen solution is not observed.

In contrast, recently time-resolved IR-studies with liquid samples showed transient formation of azide radicals upon laser photolysis at 266 nm.[11] This result shows that primary photoreduction occurs, but the corresponding $\mathrm{Fe^{II}}$ species does not accumulate over time in experiments with frozen samples. An explanation may be found in the microscopic reversibility of the reductive $N_3^{\bullet}$ radical elimination from $\mathrm{Fe^{III}N_3}$, in contrast to the irreversibility of the oxidative N_2 elimination. Thus, upon prolonged irradiation in solid matrix, the irreversible oxidative process may dominate, because the $N_3^{\bullet}$ radicals from photoreduction are prevented from diffusion so that effective recombination, $2\,N_3^{\bullet} \rightarrow 3\,N_2$, may occur. The situation may be different in solution, but a general rule cannot be derived from the present data. The conditions under which $\mathrm{Fe^{II}}$ (**1d**) or $\mathrm{Fe^{V}N}$ (**1b**) are formed may be more complicated than simply the intrinsic wavelength dependence of the primary photoprocess. In practice, the state of aggregation (fluid solution vs. frozen solution) appears to dictate the preparative yield of products.

In summary, the octahedral $\mathrm{Fe^{V}N}$ species undergoes rapid, highly exothermic nitride coupling and the formation of dinitrogen, whereas reactions with the solvent do not take place. Nitride coupling is driven by the stability of the $\mathrm{Fe^{II}}$-NN-$\mathrm{Fe^{II}}$ intermediate and is barrier-free. The reaction equilibrium is strongly on the dinitrogen side. Hence it will be challenging to push it to the nitride side for possible ammonia formation or N-functionalization of substrates from dinitrogen. Furthermore, the present study revises the previously reported wavelength dependence of the photolysis of the iron azide complex $[Fe^{III}(N_3)cyc\text{-}ac]^+$ (**1**). The yield of high- and low-valent products rather depends on the feasibility of subsequent reactions. Finally, the data revealed that similar six-coordinate structures are obtained for reduced **1d** and **2d**, with a solvent molecule bound in an axial position, independently of how the complexes have been generated, (electro)chemically, by putative photoreduction, or from $Fe^{V}N$ groups by nitride coupling.

Received: March 20, 2014

Keywords: Fe^V nitrides · iron · mass spectrometry · Mössbauer spectroscopy · nitride coupling

---

[1] B. M. Hoffman, D. R. Dean, L. C. Seefeldt, *Acc. Chem. Res.* **2009**, *42*, 609–619.

[2] a) G. Ertl, *Chem. Rec.* **2001**, *1*, 33–45; b) G. Ertl, *Angew. Chem.* **1990**, *102*, 1258–1266; *Angew. Chem. Int. Ed. Engl.* **1990**, *29*, 1219–1227.

[3] a) J. Hohenberger, K. Ray, K. Meyer, *Nat. Commun.* **2012**, *3*, 720; b) J. J. Scepaniak, C. S. Vogel, M. M. Khusniyarov, F. W. Heinemann, K. Meyer, J. M. Smith, *Science* **2011**, *331*, 1049–1052; c) C. Vogel, F. W. Heinemann, J. Sutter, C. Anthon, K. Meyer, *Angew. Chem.* **2008**, *120*, 2721–2724; *Angew. Chem. Int. Ed.* **2008**, *47*, 2681–2684; d) N. Aliaga-Alcalde, S. DeBeer George, B. Mienert, E. Bill, K. Wieghardt, F. Neese, *Angew. Chem.* **2005**, *117*, 2968–2972; *Angew. Chem. Int. Ed.* **2005**, *44*, 2908–2912; e) T. A. Betley, J. C. Peters, *J. Am. Chem. Soc.* **2004**, *126*, 6252–6254; f) C. A. Grapperhaus, B. Mienert, E. Bill, T. Weyhermüller, K. Wieghardt, *Inorg. Chem.* **2000**, *39*, 5306–5317; g) W. D. Wagner, K. Nakamoto, *J. Am. Chem. Soc.* **1989**, *111*, 1590–1598; h) J. J. Scepaniak, J. A. Young, R. P. Bontchev, J. M. Smith, *Angew. Chem.* **2009**, *121*, 3204–3206; *Angew. Chem. Int. Ed.* **2009**, *48*, 3158–3160.

[4] J. J. Scepaniak, M. D. Fulton, R. P. Bontchev, E. N. Duesler, M. L. Kirk, J. M. Smith, *J. Am. Chem. Soc.* **2008**, *130*, 10515–10517.

[5] a) J. F. Berry, E. Bill, E. Bothe, S. D. George, B. Mienert, F. Neese, K. Wieghardt, *Science* **2006**, *312*, 1937–1941; b) K. Meyer, E. Bill, B. Mienert, T. Weyhermüller, K. Wieghardt, *J. Am. Chem. Soc.* **1999**, *121*, 4859–4876.

[6] a) J. M. Smith, D. Subedi, *Dalton Trans.* **2012**, *41*, 1423–1429; b) J. F. Berry, *Comments Inorg. Chem.* **2009**, *30*, 28–66; c) C. T. Saouma, J. C. Peters, *Coord. Chem. Rev.* **2011**, *255*, 920–937.

[7] J. J. Scepaniak, R. P. Bontchev, D. L. Johnson, J. M. Smith, *Angew. Chem.* **2011**, *123*, 6760–6763; *Angew. Chem. Int. Ed.* **2011**, *50*, 6630–6633.

[8] M. P. Hendrich, W. Gunderson, R. K. Behan, M. T. Green, M. P. Mehn, T. A. Betley, C. C. Lu, J. C. Peters, *Proc. Natl. Acad. Sci. USA* **2006**, *103*, 17107–17112.

[9] J. Torres-Alacan, U. Das, A. C. Filippou, P. Vöhringer, *Angew. Chem.* **2013**, *125*, 13067–13071; *Angew. Chem. Int. Ed.* **2013**, *52*, 12833–12837.

[10] D. Schröder, H. Schwarz, N. Aliaga-Alcalde, F. Neese, *Eur. J. Inorg. Chem.* **2007**, 816–821.

[11] a) J. Torres-Alacan, O. Krahe, A. C. Filippou, F. Neese, D. Schwarzer, P. Vöhringer, *Chem. Eur. J.* **2012**, *18*, 3043–3055; b) H. Vennekate, D. Schwarzer, J. Torres-Alacan, O. Krahe, A. C. Filippou, F. Neese, P. Vohringer, *Phys. Chem. Chem. Phys.* **2012**, *14*, 6165–6172.

[12] F. Neese, *WIREs Comput. Mol. Sci.* **2012**, *2*, 73. The ORCA program is available free of charge at http://www.cec.mpg.de/downloads.html.

[13] a) A. D. Becke, *Phys. Rev. A* **1988**, *38*, 3098–3100; b) J. P. Perdew, *Phys. Rev. B* **1986**, *34*, 7406–7406; c) J. P. Perdew, *Phys. Rev. B* **1986**, *33*, 8822–8824.

[14] O. Vahtras, J. Almlof, M. W. Feyereisen, *Chem. Phys. Lett.* **1993**, *213*, 514–518.

[15] a) A. Schäfer, H. Horn, R. Ahlrichs, *J. Chem. Phys.* **1992**, *97*, 2571–2577; b) F. Weigend, R. Ahlrichs, *Phys. Chem. Chem. Phys.* **2005**, *7*, 3297–3305.

[16] a) A. Klamt, G. Schuurmann, *J. Chem. Soc. Perkin Trans. 2* **1993**, 799–805; b) A. Klamt, *J. Phys. Chem.* **1995**, *99*, 2224–2235.

[17] T. Schwabe, S. Grimme, *Phys. Chem. Chem. Phys.* **2006**, *8*, 4398–4401.

[18] a) C. T. Lee, W. T. Yang, R. G. Parr, *Phys. Rev. B* **1988**, *37*, 785–789; b) A. D. Becke, *J. Chem. Phys.* **1993**, *98*, 5648–5652.

[19] F. Neese, F. Wennmohs, A. Hansen, U. Becker, *Chem. Phys.* **2009**, *356*, 98–109.

[20] F. Neese, *Inorg. Chim. Acta* **2002**, *337*, 181–192.

[21] A. P. Scott, L. Radom, *J. Phys. Chem.* **1996**, *100*, 16502–16513.